ORIGINAL RESEARCH

The Physiological Society · american physiological society · **Physiological** Reports

Prostaglandin D$_2$ signaling is not involved in the recovery of rat hind limb tendons from injury

Dylan C. Sarver[1] | Kristoffer B. Sugg[1,2,3] (iD) | Jeffrey R. Talarek[1,2,4] | Jacob B. Swanson[4] (iD) | David J. Oliver[4] | Aaron C. Hinken[5] | Henning F. Kramer[5] | Christopher L. Mendias[1,2,4,6] (iD)

[1]Department of Orthopaedic Surgery, Section of Plastic & Reconstructive Surgery, University of Michigan Medical School, Ann Arbor, MI, USA

[2]Department of Molecular & Integrative Physiology, Section of Plastic & Reconstructive Surgery, University of Michigan Medical School, Ann Arbor, MI, USA

[3]Department of Surgery, Section of Plastic & Reconstructive Surgery, University of Michigan Medical School, Ann Arbor, MI, USA

[4]Hospital for Special Surgery, New York, NY, USA

[5]Muscle Metabolism DPU, GlaxoSmithKline Pharmaceuticals, King of Prussia, PA, USA

[6]Department of Physiology & Biophysics, Weill Cornell Medical College, New York, NY, USA

Correspondence
Christopher Mendias, Hospital for Special Surgery, 535 E 70th St, New York, NY 10021, USA.
Email: mendiasc@hss.edu

Present address
Dylan C. Sarver, Department of Physiology, Johns Hopkins University School of Medicine, Baltimore, MD, USA

Abstract

Injured tendons heal through the formation of a fibrovascular scar that has inferior mechanical properties compared to native tendon tissue. Reducing inflammation that occurs as a result of the injury could limit scar formation and improve functional recovery of tendons. Prostaglandin D$_2$ (PGD$_2$) plays an important role in promoting inflammation in some injury responses and chronic disease processes, and the inhibition of PGD$_2$ has improved healing and reduced disease burden in animal models and early clinical trials. Based on these findings, we sought to determine the role of PGD$_2$ signaling in the healing of injured tendon tissue. We tested the hypothesis that a potent and specific inhibitor of hematopoietic PGD synthase (HPGDS), GSK2894631A, would improve the recovery of tendons of adult male rats following an acute tenotomy and repair. To test this hypothesis, we performed a full-thickness plantaris tendon tenotomy followed by immediate repair and treated rats twice daily with either 0, 2, or 6 mg/kg of GSK2894631A. Tendons were collected either 7 or 21 days after surgical repair, and mechanical properties of tendons were assessed along with RNA sequencing and histology. While there were some differences in gene expression across groups, the targeted inhibition of HPGDS did not impact the functional repair of tendons after injury, as HPGDS expression was surprisingly low in injured tendons. These results indicate that PGD$_2$ signaling does not appear to be important in modulating the repair of injured tendon tissue.

KEYWORDS
GSK2894631A, HPGDS, RNA sequencing, tendon mechanics, tenotomy

Dylan C. Sarver and Kristoffer B. Sugg authors are contributed equally to this work.

1 | INTRODUCTION

Tendon is a dynamic tissue that is important for transmitting and storing elastic energy between skeletal muscle and bone. While tendon is mechanically robust, it can rupture in response to excessive strain placed on the tissue, or with repetitive high-frequency loading activities that generate a series of small tears which propagate over time (Mead, Gumucio, Awan, Mendias, & Sugg, 2018; Sharma & Maffulli, 2006). Tendon ruptures can be treated either conservatively or with surgical repair, but in both cases a fibrovascular scar forms between the torn tendon stumps (Ganestam, Kallemose, Troelsen, & Barfod, 2016; Sharma & Maffulli, 2006; Yang, Rothrauff, & Tuan, 2013). This scar tissue has inferior mechanical properties compared to native tendon tissue and disrupts the normally efficient transfer of force throughout the tendon, which leads to impaired locomotion (Freedman et al., 2017; Nourissat, Berenbaum, & Duprez, 2015; Yang et al., 2013).

There is a substantial inflammatory response that occurs in the early stages of the repair of a torn tendon, including infiltration of neutrophils and macrophages, and an upregulation in proinflammatory cytokines and cyclooxygenase (COX) enzymes (Koshima et al., 2007; Marsolais, Côté, & Frenette, 2001). Nonsteroidal anti-inflammatory drugs (NSAIDs) and COX-2 inhibitors (coxibs) have been used clinically to treat pain and prevent inflammation after tendon repair, but in most cases, the use of NSAIDs or coxibs reduces or delays tissue healing (Dimmen, Engebretsen, Nordsletten, & Madsen, 2009; Ferry, Dahners, Afshari, & Weinhold, 2007; Hammerman, Blomgran, Ramstedt, & Aspenberg, 2015). This is true not only for tendon, but also for other musculoskeletal tissues including skeletal muscle, bone, and the enthesis (Cohen, Kawamura, Ehteshami, & Rodeo, 2006; Dueweke, Awan, & Mendias, 2017; Lisowska, Kosson, & Domaracka, 2018; Su & O'Connor, 2013). NSAIDs and coxibs block the production of prostaglandin H_2 (PGH_2) from arachidonic acid (AA), and PGH_2 is a precursor for the production of several prostaglandins including PGD_2, PGE_2, $PGF_{2\alpha}$, and PGI_2 (Trappe & Liu, 2013). Although less is known for tendon, the negative effects of NSAIDs and coxibs on skeletal muscle healing are thought to occur by blocking the production of $PGF_{2\alpha}$, which is critical for muscle fiber growth and regeneration (Trappe & Liu, 2013). Therefore, developing a therapy that can specifically target proinflammatory prostaglandins without impacting other prostaglandins could improve the treatment of tendon disorders.

PGD_2 is a proinflammatory prostaglandin that is produced from PGH_2 by two enzymes, hematopoietic PGD synthase (HPGDS) and lipocalin-type PGD synthase (PTGDS) (Joo & Sadikot, 2012; Thurairatnam, 2012). HPGDS is expressed in various immune and inflammatory cells that participate in the repair of injured tissues (Thurairatnam, 2012), and the targeted inhibition of PGD_2 production improves skeletal muscle repair after injury and also reduces the pathological muscle changes in the *mdx* model of Duchenne muscular dystrophy (Mohri et al., 2009; Thurairatnam, 2012). Blocking PGD_2 production has also improved outcomes in animal models and small clinical trials of pulmonary, autoimmune, and neurodegenerative disease, among others (Thurairatnam, 2012). Based on these findings, we sought to test the hypothesis that the targeted inhibition of PGD_2 would improve tendon healing following a plantaris tenotomy and repair. To test this hypothesis, we induced an acute plantaris tendon tear followed by an immediate repair, and then treated rats twice daily with GSK2894631A to inhibit the enzymatic activity of HPGDS. Tendons were collected either 7 or 21 days after surgical repair, and mechanical properties were assessed along with transcriptional and histological measurements to determine the impact of HPGDS inhibition on tendon structure and function after tenotomy and repair.

2 | MATERIALS AND METHODS

2.1 | Animals

This study was approved by the University of Michigan IACUC (protocol PRO00006079). Three-month-old male Sprague Dawley rats were purchased from Charles River and housed under specific pathogen-free conditions. This age was selected to be reflective of early adulthood. Animals were provided food and water ad libitum. There were six experimental groups in the study, with $N = 12$ rats per group, for a total of 72 surgical rats. An additional five control rats that did not undergo tenotomy surgery or receive the test compound were used in the study to obtain reference values for assays. We estimated the sample size study based on energy absorption values from a previous study (Mendias, Roche, et al., 2015). To detect a 30% difference in energy absorption between vehicle and 6 mg/kg doses at the 7 day and 21 day time points, using a power of 80% and an alpha adjusted from .05 for multiple observations, required $N = 9$ per each surgical group. We added three additional rats to account for unanticipated losses.

2.2 | Surgical procedure and administration of test compound

All surgical procedures were performed bilaterally. Animals were deeply anesthetized with 2% isoflurane, and the skin overlying the surgical site was shaved and scrubbed with 4% chlorhexidine. The animals received a subcutaneous injection of buprenorphine (0.05 mg/kg, Reckitt Benckiser) for preoperative analgesia. A longitudinal incision was then performed within the interval between the Achilles and plantaris tendons on each

hind limb. The skin and paratenon were split and retracted to achieve optimal visualization of the plantaris tendon, which is located medial and deep to the Achilles tendon. A full-thickness tenotomy was created in the midsubstance of the plantaris tendon, followed by immediate repair using a Bunnell technique with Ethibond (5-0, Ethicon). The Achilles tendon was left intact to function as a stress shield for the repaired plantaris tendon. A splash block of 0.2 ml of 0.5% bupivacaine was administered, the paratenon was then loosely reapproximated using Vicryl suture (4-0, Ethicon), and the skin was closed with GLUture (Abbott). After recovery, ad libitum weight-bearing and cage activity were allowed, and the animals received a second injection of buprenorphine (0.05 mg/kg) 12 hr after surgery.

GSK2894631A (7-(Difluoromethoxy)-N-((trans)-4-(2-hydroxypropan-2-yl)cyclohexyl)quinoline-3-carbox-amide), which is a potent and specific inhibitor of human and rat HPGDS (Deaton et al., 2019), was synthesized and prepared by GlaxoSmithKline (King of Prussia). GSK2894631A was suspended in 0.5% hydroxypro-pyl methylcellulose: 0.1% Tween80 and delivered to rats via oral gavage twice daily at doses of 0, 2, or 6 mg/kg. Rats were randomly assigned to each group prior to the surgical intervention. Compounds were provided by GlaxoSmithKline to investigators in a blinded fashion, and identified using a single letter code.

Either 7 or 21 days after the tenotomy and repair surgery, animals were deeply anesthetized with an intraperitoneal injection of sodium pentobarbital (50 mg/kg, Vortech Pharmaceuticals). The left plantaris tendon, which was used for mechanical properties testing and histology, was removed by making a full-thickness incision proximal to the myotendinous junction and distal to the calcaneus, in order to preserve the myotendinous junction and enthesis. The left plantaris tendon was then wrapped in saline-soaked gauze, and stored at −20°C until use. The right plantaris tendon, which was used for RNA analysis, was removed by making an incision just distal to the myotendinous junction and just proximal to the calcaneus to avoid contaminating muscle or bone tissue,

snap frozen in liquid nitrogen, and stored at −20°C until use. Following removal of tendons, animals were humanely euthanized by overdose of sodium pentobarbital and induction of a bilateral pneumothorax.

2.3 | Mechanical properties measurement

Mechanical properties were measured as modified from previous studies (Mendias, Lynch, et al., 2015; Sarver et al., 2017). Prior to mechanical tests, tendons were thawed at room temperature and then placed in dish containing PBS. Braided silk suture (4-0, Ashaway Line & Twine) was attached to proximal and distal ends of the tendon using a series of square knots to allow the tendon to be attached to pins for geometric measurements, and to the mechanical properties testing apparatus, without damaging the tendon tissue. The tendon was then transferred to a custom device to measure cross-sectional area (CSA) (Figure 1a). The device consisted of a trough filled with PBS that contained a sedimentary layer of SYLGARD 184 (Dow Chemical) to allow the placement of minutien pins, to which the sutured tendon was attached. The trough was also flanked by prisms that allow for visualization of the side view of the tendon. The tendon was held at just taught length, and the CSA was calculated from five evenly spaced width and depth measurements from high-resolution digital photographs of both top and side views of the tendon. These measurements were then fit to an ellipse, and the average ellipse area was used as the tendon CSA for mechanical properties measurements.

To test mechanical properties, the tendon was then transferred to a bath containing PBS maintained at 25°C. Using the attached sutures, the distal end of the tendon was secured by affixing the calcaneus to a 10N dual-mode servomotor/force transducer (model 305LR, Aurora Scientific), while the proximal end of the tendon was secured at the myotendinous junction to a hook attached to a micropositioner (Figure 1b). Once secured, the tendon was briefly raised up from the bath so that GLUture adhesive could be applied to reinforce the attachment of the calcaneus to the hook. The tendon was
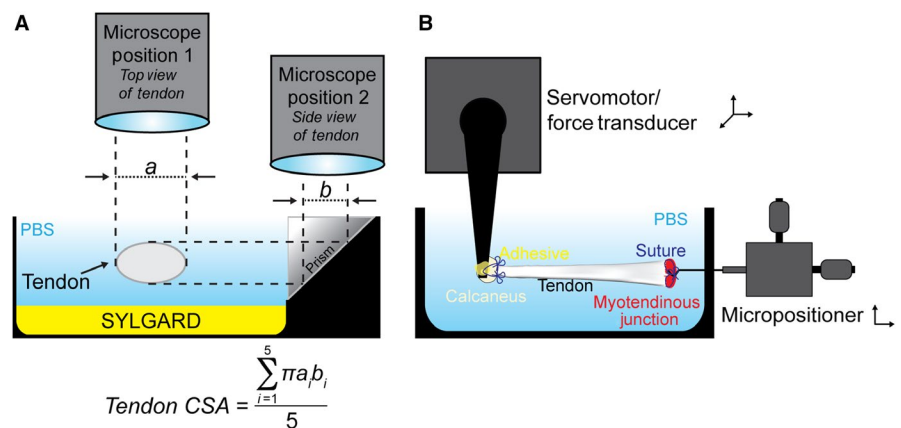
FIGURE 1 Overview of cross-sectional area and mechanical properties testing devices. (a) Schematic showing the measurement of nominal tendon cross-sectional area, with the tendon shown in cross-section. (b) Schematic showing the measurement of mechanical properties of tendons

$$Tendon\ CSA = \frac{\sum_{i=1}^{5} \pi a_i b_i}{5}$$

then returned to the bath, and its length was adjusted to an approximate 5-mN preload, which was consistent with the just taught length, and recorded as L_o. Each tendon was subjected to 10 load-unload stretch cycles at a constant velocity of 0.05 L_o/s, and a length change that was 10% of L_o. Data were recorded using custom LabVIEW software (National Instruments). Load, stress, tangent modulus, and energy loss were determined for each load-unload cycle. Tangent modulus was defined as the maximum derivative over a 10 ms window of data from the stress–strain curve. Energy loss was calculated as the area under force-displacement curve from 10% to 0% strain subtracted from the area under the force-displacement curve from 0% to 10% strain. Energy loss was then normalized by tendon mass, which was determined by multiplying the volume of tendon by 1.12 g/cm^3 (Ker, 1981).

Following the completion of mechanical properties testing, the tendon ends were trimmed, the tendon was placed in Tissue-Tek OCT Compound (Sakura Finetek), flash frozen in isopentane cooled in liquid nitrogen, and then stored at −80°C until use.

2.4 | Histology

Longitudinal sections of tendons, approximately 10 μm in thickness, were obtained using a cryostat. Sections were stained with hematoxylin and eosin, and digital images were obtained with a Nikon Eclipse microscope equipped with a high-resolution camera (Nikon).

2.5 | RNA sequencing and gene expression

RNA was extracted as modified from previous studies (Gumucio, Phan, Ruehlmann, Noah, & Mendias, 2014; Nielsen et al., 2014). Tendons were finely minced, and then placed into 2-ml tubes containing 2.3-mm steel beads and TRI Reagent (Molecular Research Center), homogenized for 15 s, and isolated following product directions. The subsequent RNA pellet was then further cleaned up using miRNeasy kit (Qiagen), supplemented with DNase I (Qiagen). RNA concentration was determined using a NanoDrop (ThermoFisher Scientific), and quality was assessed using a TapeStation D1000 System (Agilent). All RNA samples used for sequencing had RIN values >8.0.

RNA sequencing was performed by the University of Michigan sequencing core using an HiSeq 4000 system (Illumina) and TruSeq reagents (Illumina) with 50 bp single end reads as described (Disser et al., 2019; Gumucio et al., 2019). A total of 1 μg of RNA from five rats from each group was analyzed. Read quality was assessed and adapters were trimmed using fastp (Chen, Zhou, Chen, & Gu, 2018). Based on fastp quality analysis, two samples from control group, one from the 7 day GSK2894631A 2 mg group, and one from the 7 day 6 mg GSK2894631A group, were removed from further analysis. Reads were then mapped to the rat genome version RN6 and reads in exons were counted against RN6 Ensembl release 95 with STAR Aligner (Dobin et al., 2013). Differential gene expression analysis was performed in R using edgeR (Robinson, McCarthy, & Smyth, 2010). Genes with low expression levels (less than 3 counts per million mapped reads in at least one group) were filtered from all downstream analyses. A Benjamini–Hochberg false discovery rate (FDR) procedure was used to correct for multiple testing and FDR-adjusted p values less than .05 were considered significant. Sequence data was deposited to NIH GEO (accession number GSE130276).

For quantitative PCR (qPCR), RNA was first reverse transcribed into cDNA using iScript reagents (Bio-Rad). qPCR was conducted in a CFX96 real-time thermal cycler using SsoAdvanced SYBR green supermix reagents (BioRad). The $2^{-\Delta Ct}$ method was used to normalize the expression of mRNA transcripts to the stable housekeeping gene *Ppp1ca*. A listing of primer sequences is provided in Table 1.

2.6 | Statistics

Primary data were acquired in a blinded fashion. Values are presented as mean ± *SD*. Statistical analyses of RNAseq data are described above. As the mechanical properties data in this study did not follow a Gaussian distribution, differences between groups were tested using a Kruskal–Wallis test followed by a Benjamini–Krieger–Yekutieli FDR correction (α = .05) to adjust for multiple observations across groups. Gene expression, as measured by qPCR, was assessed using a Brown–Forsythe test followed by a Benjamini–Krieger–Yekutieli FDR correction (α = .05). These analyses allowed for the assessment of differences between all treatment groups and control tendons, as well as differences within a time point and within a treatment dose. Prism (version 8.0, GraphPad) was used to perform statistical calculations.

3 | RESULTS

An overview of the surgical procedure and study groups is shown in Figure 2a–b.

All rats tolerated the surgical procedure, gavage, and drug treatment well, and there were no differences in body mass at the time of harvest (Figure 3a). As expected, the tenotomy and repair procedure resulted in inflammation and scar tissue formation, in particular around the areas of suture placement (Figure 2c–i). This resulted in an approximate 6-fold increase in the nominal CSA of tendons across all repaired groups (Figure 3b). While the tendons became enlarged, no apparent gross differences in histological features were noted between the three treatment groups at either the 7 or 21 days time points (Figure 2d–i).

TABLE 1 qPCR Primers. Sequences of primers used for qPCR

| Symbol	Description	GenBank ID	Forward Primer (5' to 3')	Reverse Primer (5' to 3')	Size (bp)
Ccl2	Chemokine (C-C motif) ligand 2	NM_031530.1	TAGCATCCACGTGCTGTCTC	CAGCCGACTCATTGGGATCA	94
Cd11b	Integrin alpha M/Cd11b	NM_012711	AAGCAGAATTTCGGTGCCTG	TGGTATTGCCATCAGCGTCC	112
Cd163	Cluster of differentiation molecule 163	NM_001107887.1	TGTAGTTCATCATCTTCGGTCCAA	CCAAGCGGAGTTGACCACTT	91
Col1a1	Collagen, type I, alpha 1	NM_053304	ATCAGCCCAAACCCAAGGAGA	CGCAGGAAGGTCAGCTGGATAG	128
Col3a1	Collagen, type III, alpha 1	NM_032085	TGATGGGGATCCAATGAGGGAGA	GAGTCTCATGGCCTTGCGTGTTT	143
Hmmr	CD168, Hyaluronan mediated motility rcptr	NM_012964	ACGAAGTCAACTGCGGAACA	TGCGCTGTGTCACTGTACTT	134
Hpgds	Hematopoietic prostaglandin D synthase	NM_031644	TGGATGCAGTGGTGGATACC	GATGAGGTGCTTGACGTGTGA	117
Ppp1ca	Protein phosphatase 1 catalytic subunit alpha	NM_031527.1	ACAGCGAGAAGCTCAACCTG	AGGCAAAGACCACGGATCTC	112
Ptgds	Prostaglandin D2 synthase	NM_013015.2	TACGATGAGTACGCGTTCCTG	CCTGGTCCTTGCTAAAGGTGA	139
Ptges	Prostaglandin E synthase	NM_021583.3	ACCCTCTCATCGCCTGGATA	CGTGGGTTCATTTTGCCCAG	88
Ptgs1	Prostaglandin-endoperoxide synthase 1/ COX1	NM_017043.4	CCCACCTTCCGTAGAACAGG	GAGCAACCCAAACACCTCCT	100
Ptgs2	Prostaglandin-endoperoxide synthase 2/ COX2	NM_017232.3	GTGGAAAAGCCTCGTCCAGA	TCCTCCGAAGGTGCTAGGTT	132
Scx	Scleraxis	NM_001130508.1	CCACTCCAGTCCGAACACAT	TCATGCCGCCTCTTTAGGTC	108
Tnmd	Tenomodulin	NM_022290.1	CACTGGCATCTACTTTGTAGGTCT	GCAGGAACCCAAATCACTGAC	150
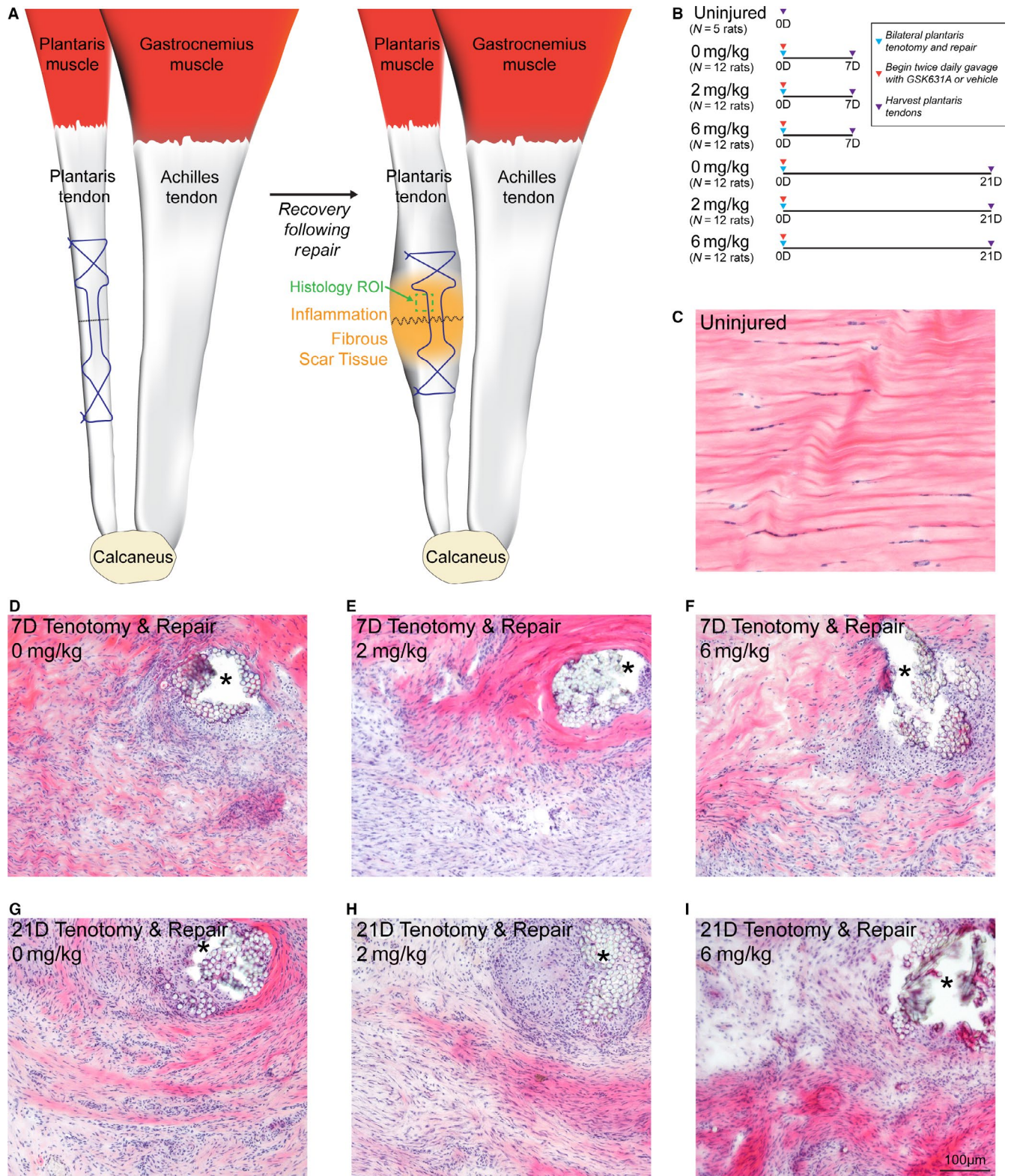
FIGURE 2 Overview of acute tenotomy and repair procedure, and representative histology of repaired plantaris tendons. (a) Overview of the surgical procedure, demonstrating a tenotomy (dashed black line) and Bunnell repair technique (suture pattern shown in blue) of the plantaris tendon. After the animals recover, inflammation and fibrous scar tissue will accumulate in the area of injury. The representative region of interest (ROI) for histology panels (c–i) is shown in green. (b) Overview of the study design and groups. (c–i) Hematoxylin and eosin histology stained sections from the midsubstance of plantaris tendons from (c) uninjured rats, and from rats treated with 0, 2, or 6 mg/kg of GSK2894631A taken either 7 days (d–f) or 21 days (g–i) after acute tenotomy and repair. Areas of suture or suture resorption are shown with an asterisk. Scale bar for all histological sections is 100 μm
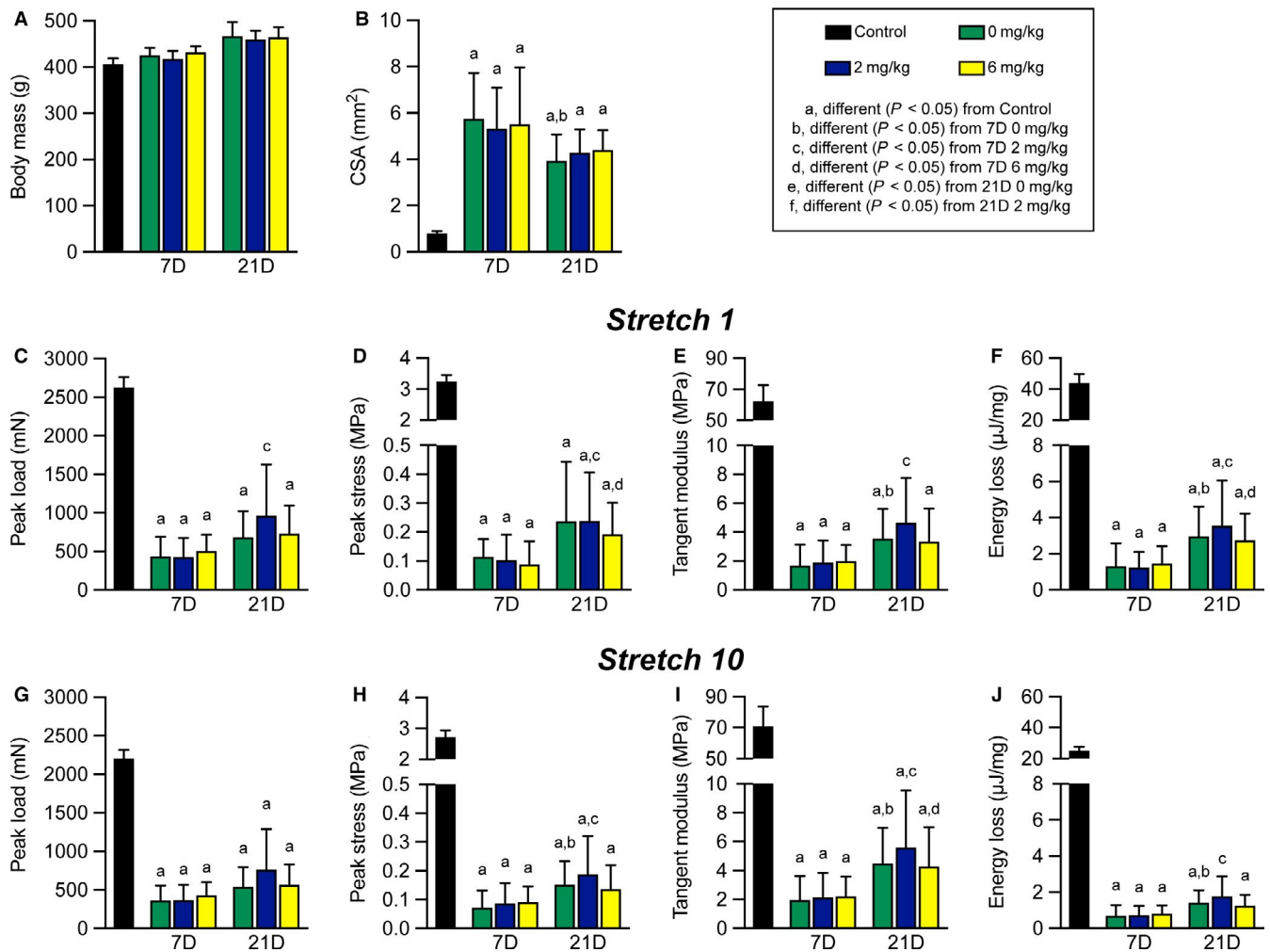
FIGURE 3 Mechanical properties of repaired plantaris tendons. (a) Animal body mass at the time of sacrifice, and (b) nominal cross-sectional area (CSA) of plantaris tendons. (c) Peak load, (d) peak stress, (e) tangent modulus, and (f) energy loss of tendons from the first of ten stretch cycles. (g) Peak load, (h) peak stress, (i) tangent modulus, and (j) energy loss of tendons from the last of ten stretch cycles. Values presented as mean $\pm$ *SD*. Differences between groups were assessed using a Kruskal–Wallis test followed by a Benjamini–Krieger–Yekutieli FDR correction ($\alpha = .05$) to identify post-hoc differences between groups: a, different (FDR-adjusted $p < .05$) from control tendons; b, different (FDR-adjusted $p < .05$) from 7D 0 mg/kg; c, different (FDR-adjusted $p < .05$) from 7D 2 mg/kg; d, different (FDR-adjusted $p < .05$) from 7D 6 mg/kg; e, different (FDR-adjusted $p < .05$) from 21D 0 mg/kg; f, different (FDR-adjusted $p < .05$) from 21D 2 mg/kg. $N = 5$ tendons for controls, and $N = 12$ tendons for each surgical repair group

Mechanical properties testing was used to assess the functional impact of HPGDS inhibition on tendon repair, shown in Figure 3c–j. Tendons were stretched for 10 cycles with a total displacement of 10% original length (L_o), and destructive testing was not performed to allow tendons to be preserved for histology. Broadly comparing control tendons to all repaired groups, peak load values were reduced by about 76% (Figure 3c and g), which is consistent with the observed disruptions to collagen fibrils in repaired tendons (Figure 2c–i). Peak stress was also lower in repaired groups by nearly 95% compared to uninjured tendons (Figure 3d and h), which is due to the reduction in peak load and the increase in CSA in repaired tendons (Figure 3b, c, and g). Tangent modulus and energy loss had similar reductions (Figure 3e, f, i, and j), likely due to an accumulation of fibrotic scar tissue (Figure 2c–i).

Comparing within repaired tendon treatment groups, the nominal CSA of tendons across the 21D time point was about 24% lower than the 7D group (Figure 3b). There were no differences across time between the CSA of the three drug treatment groups, except for the 21D 0 mg/kg group which was 32% smaller than 7D 0 mg/kg tendons (Figure 3b). No differences in peak load at cycle 1 were observed across groups within a time point, although the 21D 2 mg/kg group was about 2-fold higher than the 7D 2 mg/kg group (Figure 3c). For peak stress, the 21D 0 mg/kg and 21D 2 mg/kg groups were about 2.3-fold higher than the corresponding 7D groups (Figure 3d). Tangent modulus and energy loss were not different between groups at a given time point, but for tangent modulus was 2-fold higher for the 21D 0 mg/kg and 2 mg/kg groups than they were at 7D, and for energy loss was 2.3-fold higher in all 21D groups compared
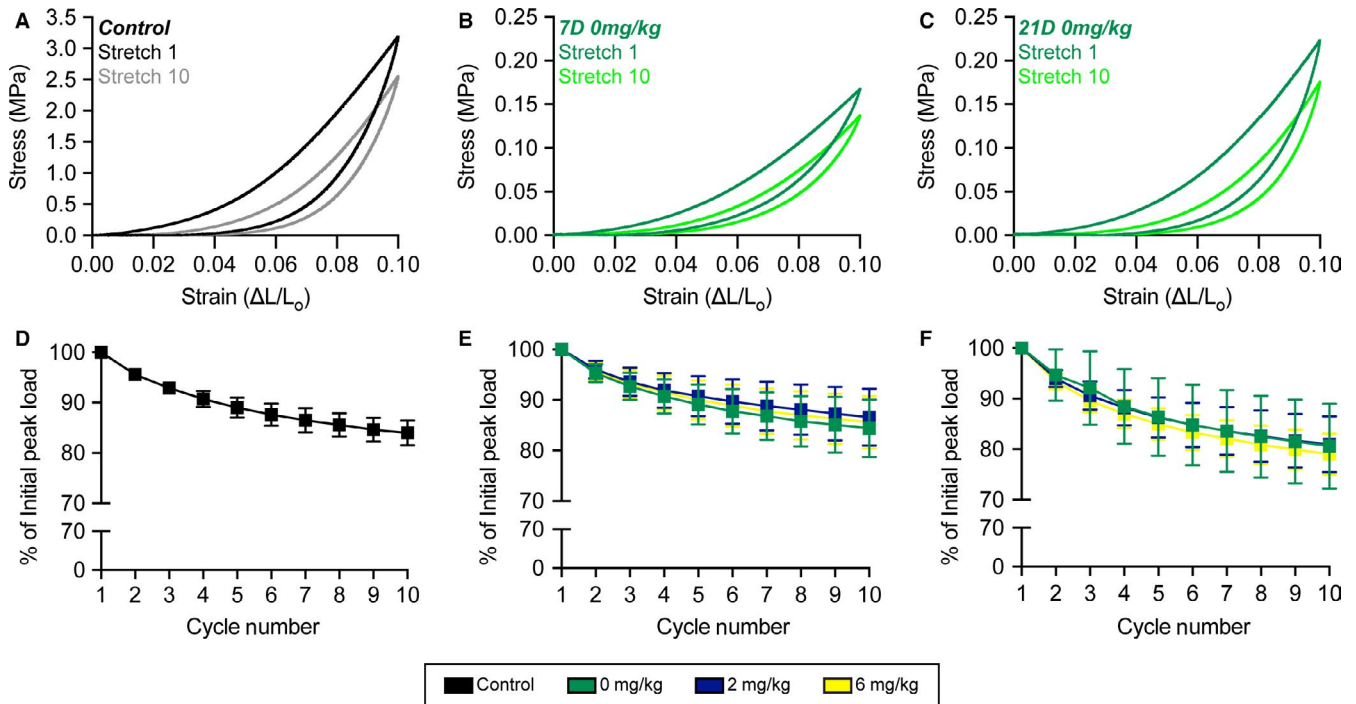
FIGURE 4 Stress–strain curves and peak load changes during stretch. Representative stress–strain response of a (a) control tendon, and (b) 7D 0 mg/kg GSK2894631A (c) 21D 0 mg/kg GSK2894631A repaired tendons from cycles 1 (darker color) and 10 (lighter color). Change in peak load across the ten cycles from (d) control tendons, and (e) 7D and (f) 21D repair groups

to 7D tendons (Figure 3e–f). The results for changes in peak load, peak stress, tangent modulus, and energy loss at stretch 10 were generally similar to observations at stretch 1 (Figure 3c–j). Although the mechanical properties of repaired tendons across time points and treatment groups were inferior to uninjured

tendons, the general shape of the stress–strain relationship remained similar (Figure 4a–c), and maintained a smooth morphology throughout the stretches indicating a relatively stiff repair callous. No differences in the shape of the stress–strain response was observed between treatment groups at a given
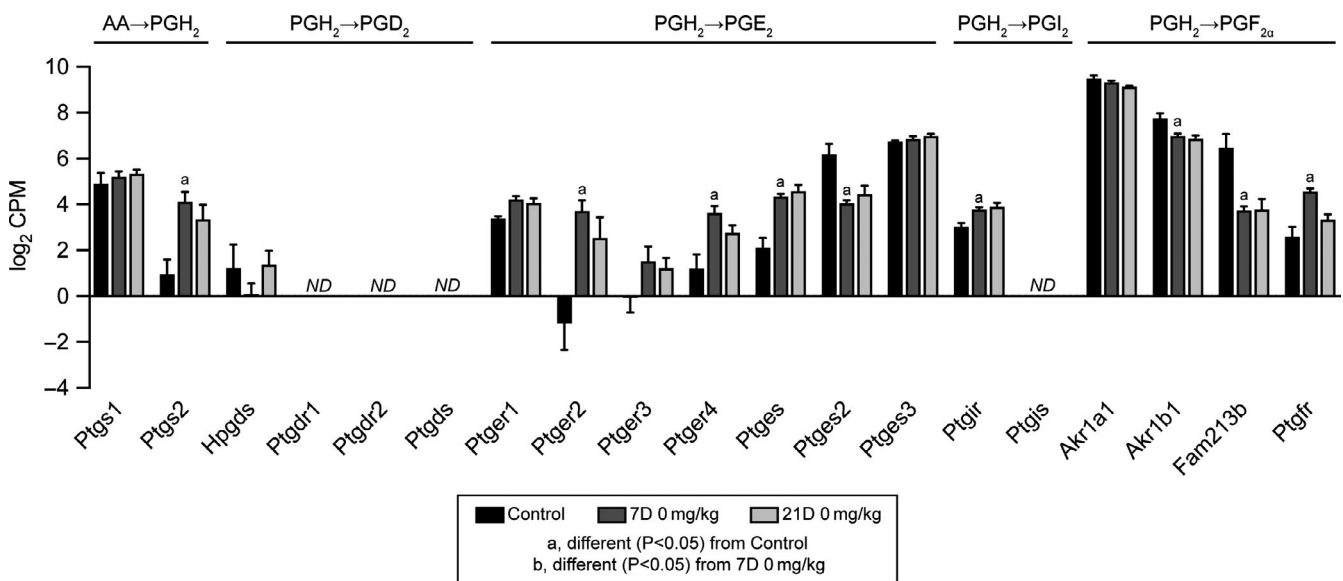
FIGURE 5 Prostaglandin synthesis RNAseq data. Expression in $\log_2$ counts per million mapped reads (CPM) for transcripts involved in the conversion of arachidonic acid (AA) to prostaglandin H_2 (PGH_2), and those which are involved in the conversion of PGH_2 into PGD_2, PGI_2, and $PGF_{2\alpha}$, as well as the receptors for these prostaglandins. Values presented as mean $\pm$ SD. Differences between groups tested with a FDR-adjusted t-test: a, different (FDR-adjusted $p < .05$) from control tendons; b, different (FDR-adjusted $p < .05$) from 7D 0 mg/kg. $N = 3$–5 tendons per group. ND, transcript not detected

time point, and we therefore only present the 0 mg/kg group to represent the shape of the curves at each time point (Figure 4b–c). The loss in force over 10 stretch cycles was also generally similar between control tendons (Figure 4d), and in the treatment groups at the 7D and 21D time points (Figure 4e–f).

We then performed RNA sequencing to comprehensively evaluate changes in transcript abundance. We first evaluated expression of genes involved in producing and sensing various prostaglandins in control and in 7D and 21D 0 mg/kg groups. Plantaris tendons express *Ptgs1* and *Ptgs2*, which convert AA into PGH_2, in control and injured tendons (Figure 5). Tendons also robustly express enzymes which convert PGH_2 into either PGE_2 or $PGF_{2\alpha}$, as well as the receptors to sense these prostaglandins (Figure 5). However, for PGD_2, *Hpgds* was expressed at a low level and *Ptgds* was not detectable, nor were the PGD_2 receptors, *Ptgdr1* and *Ptgdr2* (Figure 5). *Ptgis* which converts PGH_2 into PGI_2 was not expressed in tendons, although the receptor *Ptgir* was expressed (Figure 5).

Finally, we analyzed global changes in RNAseq values. There were 3,484 transcripts that had a FDR-adjusted *p*-value less than .05 ($-\log_{10}p$ greater than 1.3) and were at least 1.5-fold

upregulated ($\log_2$ fold change greater than 0.584) in 7D 0 mg/kg tendons compared to controls, and 3,222 transcripts that were significantly different ($-\log_{10}p$ greater than 1.3) and were at least 1.5-fold downregulated ($\log_2$ fold change less than −0.584) in the 7D 0 mg/kg group with respect to the control group (Figure 6a). By 21 days, only 82 transcripts were significantly upregulated and 43 were significantly downregulated compared to controls (Figure 6b). We then selected transcripts related to tendon healing and inflammation for further analysis across treatment groups and time points. Overall there appeared to be an effect of time since repair but not GSK2894631A treatment on regulating gene expression. For immune cell markers, compared to control tendons, there was a general increase in the myeloid cell marker *Itgax*, the macrophage recruitment gene *Ccl2*, the pan-macrophage marker *Adgre1*, M1 macrophage markers *Ccr7* and *Cd68*, T cell markers *Cd3e* and *Cd8*, and the B cell marker *Ptprc* at 7 days, but the M2 macrophage markers *Cd163*, *Hmmr*, and *Mrc1* were not different (Figure 6c). *Ptgs2*, which is involved in the synthesis of PGH_2, and *Ptges*, which catalyzes PGH_2 into PGE_2, were upregulated, while another PGE_2 synthesis enzyme, *Ptges2*, was generally downregulated 7 days after injury (Figure
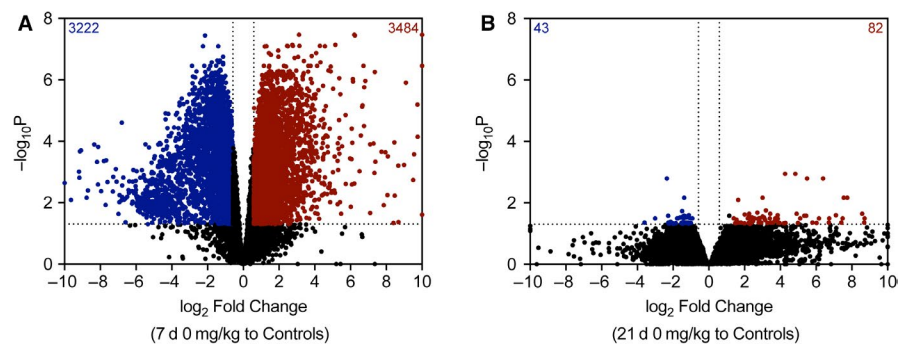
FIGURE 6 Overall RNAseq data. Volcano plots demonstrating $\log_2$ fold change and -log10 FDR-adjusted *p*-values of transcripts in the (a) 7D 0 mg/kg GSK2894631A and (b) 21D 0 mg/kg GSK2894631A groups, compared to control tendons. Heatmaps demonstrating expression of selected transcripts that are (c) inflammatory cells markers, (d) prostanoid metabolism genes, (e) involved in ECM synthesis and remodeling, (f) growth factors and cytokines, and (g) markers of tenogenesis. Data are $\log_2$ fold change in expression of each treatment group normalized to control tendons. Differences between groups tested with a FDR-adjusted *t*-test: a, different (FDR-adjusted $p < .05$) from control tendons; b, different (FDR-adjusted $p < .05$) from 7D 0 mg/kg; c, different (FDR-adjusted $p < .05$) from 7D 2 mg/kg; d, different (FDR-adjusted $p < .05$) from 7D 6 mg/kg; e, different (FDR-adjusted $p < .05$) from 21D 0 mg/kg; f, different (FDR-adjusted $p < .05$) from 21D 2 mg/kg. $N = 3$–5 tendons per group
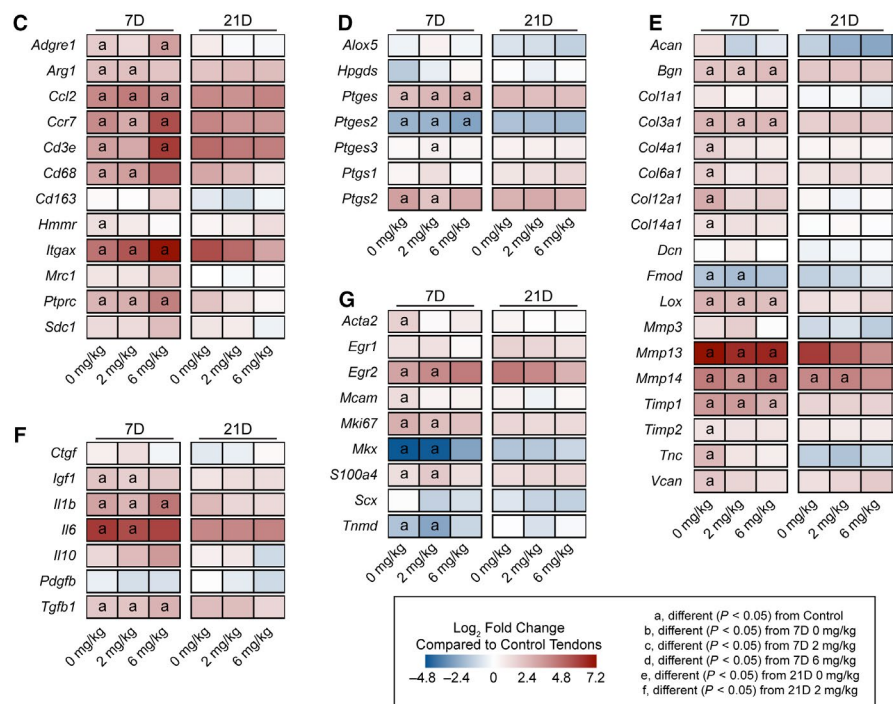
6d). The ECM genes *Col4a1*, *Col6a1*, *Col12a*, and *Col14a1*, *Tnc* and *Vcan* were upregulated in 7D 0 mg/kg tendons compared to controls, while *Col3a1* and the proteoglycans *Bgn* and *Fmod* were induced across treatment groups at 7 days (Figure 6e). *Mmp13* was upregulated in all 7 day groups, as was *Mmp14* which was also upregulated in the 21D 0 mg/kg and 2 mg/kg groups (Figure 6e). The growth factors *Igf1* and *Tgfb1* were upregulated in some of the 7-day groups compared to control tendons, as was the proinflammatory cytokine *Il1b* (Figure 6f). The early tenogenesis marker *Egr2* was generally upregulated at 7 days, while *Scx* was not different at any time point, and late tenogenesis markers, *Mkx* and *Tnmd*, were generally downregulated 7 days after injury (Figure 6g). Additionally, the myofibroblast marker *Acta2* and the tenocyte progenitor cell marker *Mcam* were upregulated in 7D 0 mg/kg tendons (Figure 6g). We also performed qPCR to analyze select genes from injured tendons, and similar to RNAseq, we generally observed very few differences between treatment groups at given time points (Table 2).

4 | DISCUSSION

Tendon tears in adult animals heal through the formation of a fibrovascular scar, with inferior mechanical properties that disrupt proper force transmission, limit performance, and increase the susceptibility for a reinjury (Freedman et al., 2017; Nourissat et al., 2015; Yang et al., 2013). Inflammation is a hallmark of tendon tears, and various prostaglandins are produced throughout the stages of tendon injury and repair (Su & O'Connor, 2013). PGD_2 plays a role in promoting inflammation in various

diseases, including skeletal muscle and nerve injury, and the inhibition of PGD_2 production has produced promising results in animal models and early clinical trials (Santus & Radovanovic, 2016; Thurairatnam, 2012). Given these encouraging findings, we tested the hypothesis that a potent and specific inhibitor of PGD_2 synthesis, GSK2894631A, would improve the recovery of tendons following an acute injury and repair. Although the test compound was well tolerated, and a handful of genes were differentially regulated across treatment groups, the targeted inhibition of PGD_2 did not impact the functional repair of tendons after injury.

NSAIDs and coxibs, which inhibit the production of PGH_2 from AA, are used to treat pain and inflammation after tendon injury. However, many studies have shown that the use of these drugs reduces or delays tendon healing (Dimmen et al., 2009; Ferry et al., 2007; Hammerman et al., 2015), which is similar to observations in other musculoskeletal tissues (Cohen et al., 2006; Dueweke et al., 2017; Lisowska et al., 2018; Su & O'Connor, 2013). PGH_2 is metabolized by specific synthases to produce other prostaglandins, such as PGD_2, PGE_2, $PGF_{2\alpha}$, and PGI_2, that modulate inflammation (Trappe & Liu, 2013). PGD_2 plays an important role in promoting inflammation, and inhibiting the HPGDS and PTGDS enzymes which produce PGD_2 from PGH_2 generally results in favorable clinical outcomes (Santus & Radovanovic, 2016; Thurairatnam, 2012).

In the current study, we found that inhibiting HPGDS had no appreciable effect on the recovery of tendon from injury. HPGDS is expressed in various immune cells, such as Th2 lymphocytes,

TABLE 2 qPCR. Gene expression in injured tendons. Target genes are normalized to the stable housekeeping gene *Ppp1ca*

Gene	7D			21D		
	0 mg/kg	2 mg/kg	6 mg/kg	0 mg/kg	2 mg/kg	6 mg/kg
Ccl2	1.90 ± 0.83	1.41 ± 0.65	1.33 ± 0.57	1.01 ± 0.47	0.98 ± 0.47	1.02 ± 0.52
Cd11b	0.15 ± 0.05	0.14 ± 0.09	0.12 ± 0.03	0.10 ± 0.14	0.08 ± 0.06	0.05 ± 0.02[c]
Cd163	0.26 ± 0.09	0.21 ± 0.08	0.27 ± 0.07	0.07 ± 0.03[a]	0.05 ± 0.02[b]	0.09 ± 0.04[c]
Col1α1	196 ± 39.0	197 ± 60.0	186 ± 33.0	125 ± 60.0	118 ± 32.0	138 ± 57.0
Col3α1	410 ± 133	447 ± 176	353 ± 108	252 ± 112	316 ± 151	374 ± 192
Hmmr	0.04 ± 0.01	0.03 ± 0.01	0.03 ± 0.01	0.02 ± 0.01[a]	0.02 ± 0.01	0.03 ± 0.01
Hpgds	0.03 ± 0.03	0.03 ± 0.01	0.02 ± 0.01	0.02 ± 0.01	0.02 ± 0.01	0.02 ± 0.01
Ptgds	ND	ND	ND	ND	ND	ND
Ptges	0.14 ± 0.04	0.13 ± 0.04	0.14 ± 0.04	0.07 ± 0.03	0.07 ± 0.02	0.09 ± 0.03
Ptgs1	0.06 ± 0.02	0.07 ± 0.02	0.05 ± 0.02	0.04 ± 0.03	0.05 ± 0.06	0.04 ± 0.02
Ptgs2	0.04 ± 0.02	0.02 ± 0.01	0.02 ± 0.01	0.01 ± 0.01	0.01 ± 0.01	0.01 ± 0.00
Scx	0.03 ± 0.03	0.03 ± 0.01	0.02 ± 0.01	0.02 ± 0.02	0.01 ± 0.01	0.02 ± 0.01
Tnmd	0.62 ± 0.43	0.40 ± 0.12	0.42 ± 0.20	0.96 ± 0.63	0.58 ± 0.28	0.87 ± 0.46

Values presented as mean ± *SD*. Differences between groups were assessed using a Brown–Forsythe test followed by a Benjamini–Kriege–Yekutieli FDR correction ($\alpha = .05$) to identify post-hoc differences between groups: a, different (FDR-adjusted $p < .05$) from 7D 0 mg/kg; b, different (FDR-adjusted $p < .05$) from 7D 2 mg/kg; c, different (FDR-adjusted $p < .05$) from 7D 6 mg/kg; d, different (FDR-adjusted $p < .05$) from 21D 0 mg/kg; e, different (FDR-adjusted $p < .05$) from 21D 2 mg/kg. $N = 6$ tendons per group. ND, not detected.

antigen-presenting cells, macrophages, mast cells, megakaryocytes, and eosinophils (Kern et al., 2017; Thurairatnam, 2012), and while little is known about the adaptive immune response in tendon, macrophages are known to accumulate after tendon injury (Marsolais et al., 2001; Sugg, Lubardic, Gumucio, & Mendias, 2014). We evaluated the expression of several markers of macrophages and adaptive immune cells, and although we generally observed an upregulation in these markers after injury, HPGDS was detected at a low level in tendon tissue and was surprisingly downregulated in most groups after injury, while other enzymes involved with prostaglandin synthesis, such as PTGES and PTGS2, were upregulated in injured tendons. The two receptors for PGD_2, PTGDR1 and PTGDR2, were also not detected in any tendon samples, indicating that if PGD_2 was produced by an unknown pathway that tendon would still likely not respond to the presence of PGD_2. There was no clear pattern for the effect of HPGDS inhibitor treatment on growth factors, cytokines, ECM components, or tenocyte markers. Combined, these results suggest that GSK2894631A does not impact tendon healing in a positive or negative manner, likely due to the absence of PGD_2-producing enzymes and PGD_2 receptors in healing tendon tissue.

There are several limitations to this work. We only evaluated two time points, chosen to be representative of the late inflammatory phase (7 days) and well into the proliferative and regenerative phases of tendon healing (21 days), and it is possible that PGD_2-producing enzymes are expressed later and have a role in modulating late stages of tendon healing. It is also possible that PGD_2-producing enzymes are expressed earlier in the repair process, but even if they are, any effects that would have occurred early on would not seem to have any impact on functional healing at later stages. Only male rats were evaluated in this study, as tendon ruptures occur three times more frequently in men than women (Ganestam et al., 2016); however, we think the results are likely applicable to both males and females. We measured transcriptional changes with RNAseq and qPCR but did not measure proteomic changes in tendons, and changes in transcript levels may not reflect changes in protein abundance. Finally, while we analyzed PGD_2 biology in plantaris tendons of rats, it is possible that other tendons, or even different species or strains of rats, do express HPGDS at a higher level, and that there could be a therapeutic role for a PGD_2 inhibitor in these instances.

5 | CONCLUSION

In the current study, based on exciting reports from other tissues and conditions, we tested the hypothesis that the targeted inhibition of HPGDS would improve the recovery of tendons from an acute plantaris tenotomy and repair. The findings of this study have lead us to reject this hypothesis, as inhibiting PGD_2 did not affect tendon healing, likely due to the low abundance of HPGDS after injury.

Although this is a negative finding, we still think this can inform the potential clinical use of PGD_2 inhibitors. While we used an acute injury model in this study, chronic tendon tears often result in substantial muscle atrophy (Davies et al., 2015; Davis, Stafford, Jergenson, Bedi, & Mendias, 2015), and there are compelling data that inhibiting PGD_2 can improve the recovery of skeletal muscle after injury and protect against atrophy (Mohri et al., 2009; Thurairatnam, 2012). Therefore, blocking PGD_2 production in a way that improves muscle healing without impacting tendon could improve upon the current clinically available prostaglandin synthase inhibitors, NSAIDs and coxibs, which generally delay healing and result in inferior functional outcomes for both muscle and tendon tissue.

CONFLICT OF INTEREST

HFK and ACH are employees of GlaxoSmithKline, which holds a patent for the GSK2894631A compound evaluated in this study. CLM has received compensation as a consultant for GlaxoSmithKline. The authors otherwise have no disclosures to report.

AUTHOR CONTRIBUTIONS

DCS, KBS, HFK, ACH, and CLM designed research; DCS, KBS, JRT, JBS, DO, and CLM performed research; DCS, KBS, JRT, JBS, DO, and CLM analyzed data; HFK and ACH contributed critical reagents; DCS, KBS, DO, and CLM wrote the paper. All authors reviewed and approved the final version of the manuscript.

ORCID

Kristoffer B. Sugg (iD) https://orcid.org/0000-0002-0301-4083
Jacob B. Swanson (iD) https://orcid.org/0000-0003-4658-2037
Christopher L. Mendias (iD) https://orcid.org/0000-0002-2384-0171

REFERENCES

Chen, S., Zhou, Y., Chen, Y., & Gu, J. (2018). fastp: An ultra-fast all-in-one FASTQ preprocessor. *Bioinformatics*, *34*, i884–i890. https://doi.org/10.1093/bioinformatics/bty560

Cohen, D. B., Kawamura, S., Ehteshami, J. R., & Rodeo, S. A. (2006). Indomethacin and celecoxib impair rotator cuff tendon-to-bone healing. *American Journal of Sports Medicine*, *34*, 362–369. https://doi.org/10.1177/0363546505280428

Davies, M. R., Ravishankar, B., Laron, D., Kim, H. T., Liu, X., & Feeley, B. T. (2015). Rat rotator cuff muscle responds differently from hindlimb muscle to a combined tendon-nerve injury. *Journal of Orthopaedic Research*, *33*, 1046–1053. https://doi.org/10.1002/jor.22864

Davis, M. E., Stafford, P. L., Jergenson, M. J., Bedi, A., & Mendias, C. L. (2015). Muscle fibers are injured at the time of acute and chronic rotator cuff repair. *Clinical Orthopaedics and Related Research*, *473*, 226–232. https://doi.org/10.1007/s11999-014-3860-y

Deaton, D. N., Do, Y., Holt, J., Jeune, M. R., Kramer, H. F., Larkin, A. L., … Saxty, G. (2019). The discovery of quinoline-3-carboxamides as hematopoietic prostaglandin D synthase (H-PGDS) inhibitors. *Bioorganic & Medicinal Chemistry*, *27*, 1456–1478. https://doi.org/10.1016/j.bmc.2019.02.017

Dimmen, S., Engebretsen, L., Nordsletten, L., & Madsen, J. E. (2009). Negative effects of parecoxib and indomethacin on tendon healing: An experimental study in rats. *Knee Surgery, Sports Traumatology, Arthroscopy*, *17*, 835–839. https://doi.org/10.1007/s00167-009-0763-7

Disser, N. P., Sugg, K. B., Talarek, J. R., Sarver, D. C., Rourke, B. J., & Mendias, C. L. (2019). Insulin-like growth factor 1 signaling in tenocytes is required for adult tendon growth. *The FASEB Journal*, *33*, 12680–12695. https://doi.org/10.1096/fj.201901503R

Dobin, A., Davis, C. A., Schlesinger, F., Drenkow, J., Zaleski, C., Jha, S., … Gingeras, T. R. (2013). STAR: Ultrafast universal RNA-seq aligner. *Bioinformatics*, *29*, 15–21. https://doi.org/10.1093/bioinformatics/bts635

Dueweke, J. J., Awan, T. M., & Mendias, C. L. (2017). Regeneration of skeletal muscle after eccentric injury. *Journal of Sport Rehabilitation*, *26*, 171–179.

Ferry, S. T., Dahners, L. E., Afshari, H. M., & Weinhold, P. S. (2007). The effects of common anti-inflammatory drugs on the healing rat patellar tendon. *American Journal of Sports Medicine*, *35*, 1326–1333. https://doi.org/10.1177/0363546507301584

Freedman, B. R., Fryhofer, G. W., Salka, N. S., Raja, H. A., Hillin, C. D., Nuss, C. A., … Soslowsky, L. J. (2017). Mechanical, histological, and functional properties remain inferior in conservatively treated Achilles tendons in rodents: Long term evaluation. *Journal of Biomechanics*, *56*, 55–60. https://doi.org/10.1016/j.jbiomech.2017.02.030

Ganestam, A., Kallemose, T., Troelsen, A., & Barfod, K. W. (2016). Increasing incidence of acute Achilles tendon rupture and a noticeable decline in surgical treatment from 1994 to 2013. A nationwide registry study of 33,160 patients. *Knee Surgery, Sports Traumatology, Arthroscopy*, *24*, 3730–3737. https://doi.org/10.1007/s00167-015-3544-5

Gumucio, J. P., Phan, A. C., Ruehlmann, D. G., Noah, A. C., & Mendias, C. L. (2014). Synergist ablation induces rapid tendon growth through the synthesis of a neotendon matrix. *Journal of Applied Physiology*, *117*, 1287–1291. https://doi.org/10.1152/japplphysiol.00720.2014

Gumucio, J. P., Qasawa, A. H., Ferrara, P. J., Malik, A. N., Funai, K., McDonagh, B., & Mendias, C. L. (2019). Reduced mitochondrial lipid oxidation leads to fat accumulation in myosteatosis. *The FASEB Journal*, *33*, 7863–7881. https://doi.org/10.1096/fj.201802457RR

Hammerman, M., Blomgran, P., Ramstedt, S., & Aspenberg, P. (2015). COX-2 inhibition impairs mechanical stimulation of early tendon healing in rats by reducing the response to microdamage. *Journal of Applied Physiology*, *119*, 534–540. https://doi.org/10.1152/japplphysiol.00239.2015

Joo, M., & Sadikot, R. T. (2012). PGD synthase and PGD2 in immune response. *Mediators of Inflammation*, *2012*, 503128–503136.

Ker, R. F. (1981). Dynamic tensile properties of the plantaris tendon of sheep (Ovis aries). *Journal of Experimental Biology*, *93*, 283–302.

Kern, K., Pierre, S., Schreiber, Y., Angioni, C., Thomas, D., Ferreirós, N., … Scholich, K. (2017). CD200 selectively upregulates prostaglandin E2 and D2 synthesis in LPS-treated bone marrow-derived macrophages. *Prostaglandins & Other Lipid Mediators*, *133*, 53–59. https://doi.org/10.1016/j.prostaglandins.2017.06.002

Koshima, H., Kondo, S., Mishima, S., Choi, H.-R., Shimpo, H., Sakai, T., & Ishiguro, N. (2007). Expression of interleukin-1beta, cyclooxygenase-2, and prostaglandin E2 in a rotator cuff tear in rabbits. *Journal of Orthopaedic Research*, *25*, 92–97.

Lisowska, B., Kosson, D., & Domaracka, K. (2018). Positives and negatives of nonsteroidal anti-inflammatory drugs in bone healing: The effects of these drugs on bone repair. *Drug Design, Development and Therapy*, *12*, 1809–1814.

Marsolais, D., Côté, C. H., & Frenette, J. (2001). Neutrophils and macrophages accumulate sequentially following Achilles tendon injury. *Journal of Orthopaedic Research*, *19*, 1203–1209. https://doi.org/10.1016/S0736-0266(01)00031-6

Mead, M. P., Gumucio, J. P., Awan, T. M., Mendias, C. L., & Sugg, K. B. (2018). Pathogenesis and management of tendinopathies in sports medicine. *Translational Sports Medicine*, *1*, 5–13. https://doi.org/10.1002/tsm2.6

Mendias, C. L., Lynch, E. B., Gumucio, J. P., Flood, M. D., Rittman, D. S., Van Pelt, D. W., … Davis, C. S. (2015). Changes in skeletal muscle and tendon structure and function following genetic inactivation of myostatin in rats. *The Journal of Physiology*, *593*, 2037–2052. https://doi.org/10.1113/jphysiol.2014.287144

Mendias, C. L., Roche, S. M., Harning, J. A., Davis, M. E., Lynch, E. B., Sibilsky Enselman, E. R., … Bedi, A. (2015). Reduced muscle fiber force production and disrupted myofibril architecture in patients with chronic rotator cuff tears. *Journal of Shoulder and Elbow Surgery*, *24*, 111–119. https://doi.org/10.1016/j.jse.2014.06.037

Mohri, I., Aritake, K., Taniguchi, H., Sato, Y., Kamauchi, S., Nagata, N., … Urade, Y. (2009). Inhibition of prostaglandin D synthase suppresses muscular necrosis. *American Journal of Pathology*, *174*, 1735–1744. https://doi.org/10.2353/ajpath.2009.080709

Nielsen, R. H., Clausen, N. M., Schjerling, P., Larsen, J. O., Martinussen, T., List, E. O., … Heinemeier, K. M. (2014). Chronic alterations in growth hormone/insulin-like growth factor-I signaling lead to changes in mouse tendon structure. *Matrix Biology*, *34*, 96–104. https://doi.org/10.1016/j.matbio.2013.09.005

Nourissat, G., Berenbaum, F., & Duprez, D. (2015). Tendon injury: From biology to tendon repair. *Nature Reviews Rheumatology*, *11*, 223–233. https://doi.org/10.1038/nrrheum.2015.26

Robinson, M. D., McCarthy, D. J., & Smyth, G. K. (2010). edgeR: A Bioconductor package for differential expression analysis of digital gene expression data. *Bioinformatics*, *26*, 139–140.

Santus, P., & Radovanovic, D. (2016). Prostaglandin D2 receptor antagonists in early development as potential therapeutic options for asthma. *Expert Opinion on Investigational Drugs*, *25*, 1083–1092. https://doi.org/10.1080/13543784.2016.1212838

Sarver, D. C., Kharaz, Y. A., Sugg, K. B., Gumucio, J. P., Comerford, E., & Mendias, C. L. (2017). Sex differences in tendon structure and function. *Journal of Orthopaedic Research*, *35*, 2117–2126. https://doi.org/10.1002/jor.23516

Sharma, P., & Maffulli, N. (2006). Biology of tendon injury: Healing, modeling and remodeling. *Journal of Musculoskeletal and Neuronal Interactions*, *6*, 181–190.

Su, B., & O'Connor, J. P. (2013). NSAID therapy effects on healing of bone, tendon, and the enthesis. *Journal of Applied Physiology*, *115*, 892–899. https://doi.org/10.1152/japplphysiol.00053.2013

Sugg, K. B., Lubardic, J., Gumucio, J. P., & Mendias, C. L. (2014). Changes in macrophage phenotype and induction of epithelial-to-mesenchymal transition genes following acute Achilles tenotomy and repair. *Journal of Orthopaedic Research*, *32*, 944–951. https://doi.org/10.1002/jor.22624

Thurairatnam, S. (2012). Hematopoietic prostaglandin D synthase inhibitors. *Progress in Medicinal Chemistry*, *51*, 97–133.

Trappe, T. A., & Liu, S. Z. (2013). Effects of prostaglandins and COX-inhibiting drugs on skeletal muscle adaptations to exercise. *Journal of Applied Physiology*, *115*, 909–919. https://doi.org/10.1152/japplphysiol.00061.2013

Yang, G., Rothrauff, B. B., & Tuan, R. S. (2013). Tendon and ligament regeneration and repair: Clinical relevance and developmental paradigm. *Birth Defects Res C Embryo Today*, *99*, 203–222. https://doi.org/10.1002/bdrc.21041